THE UNIVERSITY OF ALBERTA

GRAIN BOUNDARY CAVITATION AND DISLOCATION CELL STRUCTURE IN FATIGUE OF NICKEL

by

© Dennis Dembicki

A THESIS

SUBMITTED TO THE FACULTY OF GRADUATE STUDIES AND RESEARCH

IN PARTIAL FULFILMENT OF THE REQUIREMENTS FOR THE DEGREE

OF MASTER OF SCIENCE

DEPARTMENT OF MINING AND METALLURGY

EDMONTON, ALBERTA

Fall, 1972

THE UNIVERSITY OF ALBERTA

FACULTY OF GRADUATE STUDIES AND RESEARCH

The undersigned certify that they have read, and recommend to the Faculty of Graduate Studies and Research, for acceptance, a thesis entitled "Grain Boundary Cavitation and Dislocation Cell Structure in Fatigue of Nickel" submitted by Dennis Dembicki in partial fulfilment of the requirements for the degree of Master of Science.

Date May 25 1972

ABSTRACT

The dislocation structures resulting from high temperature fatigue of pure nickel were studied. The test specimens were fatigued in reverse torsion at constant total strain amplitudes in an inert atmosphere of ultra-high purity nitrogen. Thin films for electron microscopy were made from specimens fatigued at 550°C and 650°C.

At 550°C and 650°C dislocation cells were observed to be rectangular and the cell walls were aligned along lines of maximum shear stresses. At 650°C the dislocation cell size was found to be a linear inverse function of the saturation stress. At 550°C and 650°C a size gradient of dislocation cells was observed near sliding grain boundaries. Small holes which may have been the result of the fatigue process were observed in some of the dislocation cell walls near the grain boundary regions.

On the basis of the above observations, a mechanism of cavity nucleation and growth is proposed. It is postulated that vacancies resulting from mechanical work are produced in the dislocation cell walls and diffuse very short distances to vacancy sinks located in the cell walls. When the rate of vacancy production exceeds the ability of the existing sinks to annihilate the vacancies produced, new sinks in the form of cavities are nucleated in the dislocation cell walls near the grain boundaries. The

proposed mechanism of grain boundary cavitation predicts that the void volume per unit weight of metal is a linear function of time for steady-state conditions.

ACKNOWLEDGEMENTS

The author is greatly indebted to Dr. F. H. Vitovec for his unfailing guidance and supervision during the course of this project and its writing. The author also wishes to thank Dr. M. L. Wayman for his assistance with electron microscopy.

The research for this thesis was supported by the National Research Council, Grant Number NRC A-2926. This support is greatly appreciated by the author.

TABLE OF CONTENTS

TABLE OF CONTENTS (Continued)

LIST OF TABLES

LIST OF FIGURES

LIST OF FIGURES (Continued)

INTRODUCTION

Fatigue is the phenomenon leading to fracture under repeated or fluctuating stresses. The number of cycles of repeated stress before failure occurs is a function of the plastic strain amplitude, the structure of the material, and the environment.

One of the most important environmental factors is temperature. At low temperatures, fatigue failure of metals generally occurs by transgranular fracture. At high temperatures (i.e., in the vicinity of one half the absolute melting point) fatigue failure of most metals occurs by nucleation and growth of cavities in the grain boundary regions leading to intergranular fracture (Fig. 1). When cavitation is occuring at grain boundaries, grain boundary migration and grain boundary sliding are also observed.[1-6]

Gifkins[7] has reviewed the current theories of nucleation of cavities on grain boundaries during creep. In fatigue, nucleation of cavities on grain boundaries appears to be a relatively easy process. Cavities can be detected after the first few percent of the fatigue life of the specimen.[1-6] Growth of cavities, rather than nucleation, is considered to be the mechanism determining the fatigue life of the specimen.

During high temperature fatigue, the grain boundaries align themselves along lines of maximum shear stresses. Westwood and Taplin[5] have shown that at high temperatures

most of the grain boundary migration occurs during the first few cycles and that the onset of cavitation coincides with the attainment of a stable grain boundary configuration. Williams and Corti[1] have demonstrated that maximum cavitation occurs on grain boundaries that experience a maximum shear stress and have attributed this to an increase in the rate of cavity nucleation resulting from an increased rate of grain boundary sliding.

The kinetics of cavity growth are generally studied by measurement of the accompanying change in density. Changes in density provide a direct and sensitive measurement of the total void volume. Gittins,[4] using this method, has made a detailed study of the kinetics of void growth in copper during high temperature fatigue. His observations are listed below:

1. Cavity growth is insignificant under conditions of elastic loading.

2. At a constant value of plastic strain amplitude, cavity volume increases linearly with time; and, at constant temperature, depends only on the plastic strain amplitude.

3. The rate of cavity growth per unit area of a grain boundary is independent of grain size.

4. At high temperatures and stresses, many small cavities are observed inside the grains.

Cyclic Stress-Strain Curves

After an initial transient behavior, a saturation or steady-state stress is usually observed in a fatigue test in which the strain amplitude is fixed. The saturation stress and the plastic strain amplitude are measured from

the height and width of the hysteresis loop (Fig. 2) produced by plotting stress versus strain.

For a given material, temperature, and cyclic frequency, a cyclic stress-strain curve (saturation stress versus plastic strain amplitude) may be obtained.[8,9] The saturation stress is usually expressed as a power law function of the plastic strain amplitude.

$$\sigma_s = \sigma_o \left(\frac{\Delta\varepsilon_p}{2\varepsilon_f}\right)^n \qquad (1)$$

where n = cyclic strain hardening exponent, $\Delta\varepsilon_p$ = plastic strain amplitude, and ε_f and σ_o are constants which Morrow[8] suggests are related to the cyclic ductility and the strength of the metal. They are probably close to the monotonic true fracture ductility and true fracture strength.

In wavy slip* metals, the saturation stress is independent of initial cold work and grain size.[8,9,11,12] At room temperature, depending on the strain amplitude and initial cold work, saturation is reached between 20% and 50% of the fatigue life of the specimen for fcc metals.[9] At high temperatures, due to diffusion controlled dislocation motion, saturation can be expected to occur much sooner than at low temperatures.

---

* metals in which screw dislocations cross-slip easily display a wavy slip mode. These materials have high stacking fault energies.
Some examples: wavy slip; Cu, Al, Fe, Ni
planar slip; Mg, Ti, Ni base superalloys

Steady-State Dislocation Structures

During fatigue of wavy slip mode metals, the saturation condition is an indication of the presence of a stable cellular dislocation structure.[10,11,13-15]

Dislocation cells have been observed in metals deformed by tensile testing, extrusion, creep and fatigue.[16-18] At room temperature, dislocation cells are not formed in metals which display a planer slip mode but are formed when these metals are deformed at high temperatures.[19] In all examples where dislocation cells have been observed, the dislocation cell size was found to be inversely proportional to the saturation or flow stress.

Staker and Holt[16] have established that the flow or saturation stress is directly proportional to the square root of the dislocation density and that the dislocation cell size is inversely proportional to the square root of the dislocation density. At constant temperature, the saturation stress is usually expressed as an inverse linear function of the dislocation cell size; that is,

$$\sigma_s = M L^{-1} \qquad (2)$$

where σ_s = saturation stress, M = constant, and L = dislocation cell size.

To establish the temperature dependence of the dislocation cell size, Staker and Holt[16] compared the normalized

flow stress* at a given temperature to the normalized flow stress at room temperature of a specimen with the same dislocation structure. The normalized flow stress was found to be less at high temperatures. This is a result of increased thermal activation at higher temperatures. They concluded that for a constant stress, as the temperature increases, the dislocation cell size increases in proportion to the amount of thermal activation.

Summary

Fatigue failure at high temperatures occurs as a result of nucleation and growth of cavities in the grain boundary regions. During fatigue of wavy slip mode metals at room temperature, dislocation cells have been observed. Dislocation cells have also been observed in a variety of other processes (e.g., creep, extrusion, tensile deformation), both at high and low temperatures.

This investigation has been planned to:

1. observe the dislocation structures resulting from high temperature fatigue,
2. compare the observed dislocation structures to those found at room temperature, and
3. observe the relation of these dislocation structures to the cavities resulting from high temperature fatigue.

---

* The flow stress was normalized by dividing the observed flow stress by the value of the shear modulus at the test temperature.

EXPERIMENTAL PROGRAM AND PROCEDURES

Experimental Program

Cyclic strain tests at different total strain amplitudes and temperatures were carried out. The testing temperatures were 550°C and 650°C.

The cyclic strain tests at high temperatures were stopped shortly after saturation so that extensive cavitation would not occur at the grain boundaries. Plastic surface replicas were made so that the extent of grain boundary migration and sliding could be observed. Thin films were then made for electron microscopy.

One test specimen was fatigued at room temperature, where cavitation is known not to occur. A thin film was prepared from this specimen for electron microscopy.

To determine the temperature dependence of the saturation stress, two specimens were fatigued at different temperatures ranging from 200°C to 700°C at a constant strain amplitude. This was done at two different strain amplitudes.

During high temperature fatigue, extensive grain boundary migration and some grain growth occurs. To determine whether these processes resulted in a prefered orientation in the surface layer of the test specimens during fatigue, one specimen was fatigued to failure at 650°C and the specimen was examined with $CuK\alpha$ X-ray radiation using a back-reflection technique on a rotating specimen.

Specimen Preparation

Pure nickel in the form of 3/4 inch rod was used to make the test specimens. The chemical analysis of the nickel is given in Table 1. Hollow torsion fatigue test specimens with an inside diameter of .250 inches and an outside diameter of .450 inches with a gage length of .500 inches were machined (Fig. 3).

Prior to testing, small surface discontinuities due to machining were removed with 600 grit emery paper. The test specimens were then electro-polished using a solution of 60% orthophosphoric acid, 30% sulfuric acid, 10% water at room temperature with an applied voltage of 8 volts and using a stainless steel cathode. They were then washed in distilled water and thoroughly dried.

Mechanical Testing

The test specimens were fatigued in a reverse torsion fatigue machine. The testing machine is shown in Fig. 4. The main parts are the drive mechanism, the specimen and grip assembly (shown separately in Fig. 5), the load cell, and the split test furnace.

The 0.25 h.p. electric motor drives an adjustable eccentric at 750 rpm. The eccentric twists the specimen and grip assembly via a connecting rod and torque arm at a preset constant stroke. The twist of the specimen test section is the total twist minus the elastic twist of the grips and drive system. The calibration for the elastic twist of the machine at various temperatures and torques

is given in Appendix I. The data for the strain amplitudes reported in this thesis were calculated from the corrected strain of the gage lengths of the test specimens. Small variations in the torque have little effect on the twist of the testing machine; therefore, the test can be considered to be a constant total (elastic plus plastic) strain amplitude type. The stresses were calculated from the measured torque considering non-linear stress-strain behavior as outlined in Appendix II.

The flat specimen heads were inserted into the slotted grips and a stainless steel atmosphere chamber was placed around the grip assembly. The grip assembly was then placed in the furnace and the atmospheric chamber was purged with ultra high purity nitrogen. The chemical analysis of the nitrogen is given in Table 2. The specimen was then brought to testing temperature and held for 30 minutes so that all temperature gradients in the assembly would stabilize and the specimens would be annealed at the testing temperature. The gas flow to the atmospheric chamber was kept at less than two cubic feet per hour.

The torque on the specimens was measured by the torsional load cell and the corresponding angle of twist was measured with a linear variable differential transducer positioned on the loading arm. The response was displayed on an oscilloscope and the resulting hysteresis was photographed using an oscilloscope camera and polaroid film.

The test specimens were fatigued up to a total of

1500 cycles. The fatigued specimens were then immediately cooled by removing the furnace and increasing the gas flow to 8 cubic feet per hour. When the specimens were cooled sufficiently, they were removed from the grip assembly and examined.

Surface Replicas

Surface replicas for optical observation were made using cellulose acetate tape and shadowing the resulting plastic replica with palladium-gold alloy. This procedure produced a flat replica of a curved surface.

Thin Film Electron Microscopy

Thin films for electron microscopy were made from the fatigued specimens. Sections of approximately .025 inches thick were cut at various angles to the central axis of the specimen with a jeweler's saw. These sections were thinned using successively finer grades of emery paper to a uniform thickness of .012 inches. Discs, three mm. in diameter, were then cut by spark machining with a standard Servo-Met spark machine with the spark intensity on range 6, using a hollow brass tool. The outside and inside surfaces of the original specimen, and hence the directions of the principal stresses, could be distinguished due to the fact that the wall thickness of the original specimens was approximately 2.5 mm. The outside surface had a convex shape and the inside surface had a concave shape. The discs were then dished using a jet electro-polishing technique. The

electrolyte used was 40% acetic acid, 30% orthophosphoric acid, 20% nitric acid, and 10% water with an applied voltage of 48 volts. Just prior to perforation, the discs were removed from the polisher and the final polishing was done using a solution of 90% acetic acid and 10% water at 25-30 volts.

The thin films thus prepared were observed in a Hitachi H.U. 11 electron microscope at 100 K.V.

Determination of Dislocation Cell Size

The average dislocation cell size in the electron micrographs were estimated using the intercept or Heyn procedure. Where a size gradient of dislocation cells was found near a grain boundary, the cell size as a function of distance from the boundary was determined by drawing parallel lines to the grain boundary at regular intervals and measuring the average width and length of the cells contained in this region.

TEST RESULTS

Cyclic strain tests were done at room temperature, 550°C, and 650°C. Plastic surface replicas were then made from the specimens which fatigued at 550°C and 650°C to evaluate the extent of grain boundary migration and sliding which occured. Extensive grain boundary migration resulted in a characteristic "square" grain boundary pattern at 550°C and 650°C. Grain boundary sliding was observed to occur along grain boundaries aligned along lines of maximum shear stresses.

Thin films were prepared from samples in which grain boundary migration and sliding occured. A thin film was also prepared from a specimen fatigued at room temperature so that the resulting dislocation structure could be directly compared to those found at high temperature.

Grain Boundary Migration and Sliding

Plastic surface replicas for optical microscopy of specimens fatigued at 550°C and 650°C are shown in Figures 6 - 8. The directions of maximum shear stresses are indicated. A well developed "square" grain boundary pattern is evident. The grain boundaries are generally aligned close to the directions of maximum shear stress.

To see if grain boundary sliding occured along grain boundaries which were aligned along lines of maximum shear stress, scratches were made on one specimen around its circumference with 600 grit emery paper. The specimen was

then fatigued and a surface replica was made (Fig. 8). The scratches, after fatigue, were wavy and discontinuous at grain boundaries, thus indicating that grain boundary sliding occured along grain boundaries which were aligned along lines of maximum shear stresses.

Room Temperature Dislocation Structures

One specimen was fatigued at room temperature to approximately 50% of the estimated fatigue life. No grain boundary migration or sliding was observed to take place. A thin film was prepared for electron microscopy. Figure 9 shows the dislocation cells which were found. The cell walls were comparatively thick and coarse. A significant dislocation density was observed in the interior of some of the dislocation cells. The alignment of the cell walls appeared to be independent of the direction of the shear stresses on the specimen. The cell walls appeared to be aligned along specific crystallographic directions in agreement with other detailed investigations of room temperature dislocation cells.[21,22]

High Temperature Dislocation Structures

Dislocation cells were observed in the specimens which were fatigued at 550°C and 650°C (Figs. 10-18). From the shape of the thin films prepared from the fatigue specimens, the direction of the maximum shear stresses in relation to the dislocation cell walls could be determined. The cell walls were found to be rectangular with the dislocation

walls aligned along lines of maximum shear stresses (Fig. 10-15). The dislocation cell walls were thinner and appeared to have a lower dislocation density than those which were observed at room temperature. This is in agreement with Shaker and Holt[16] who concluded that as the temperature was increased, the thickness of the dislocation cell walls decreased. There was no noticeable difference between the cell wall thickness at 550°C and 650°C.

Thin films were prepared from sections which were cut at 45° and parallel to the axis of the fatigue specimens. In all cases the dislocation cells were either rectangular or diamond shaped, indicating that the cellular structures observed were three dimensional arrays.

Dislocation Cell Size Gradient

Near grain boundaries which were straight and aligned along line of maximum shear, a size gradient of dislocation cells was observed (Figs. 11, 12, 13). Near grain boundaries which were not aligned along lines of maximum shear, a size gradient of dislocation cells was not observed (Fig. 14). Since maximum grain boundary sliding occurs along grain boundaries aligned along lines of maximum shear stresses,[20] it can be concluded that a size gradient of dislocation cells is formed only along those grain boundaries where appreciable sliding takes place.

Holes in Dislocation Cell Walls

In some of the dislocation cell walls which were near

the grain boundary region, small holes were observed to be present (Figs. 11, 15-18). It could not be ascertained whether these holes were the result of fatigue or preferential polishing. However, the proximity of these holes to the grain boundary, the hexagonal shape, the size, and the location of these holes in regions of high dislocation densities, suggests that these holes might be cavities which are the result of fatigue. These holes were not observed in specimens fatigued at room temperature.

Microstructure of a Failed Specimen

Figure 19 is a micrograph of a specimen in which failure occured as a result of grain boundary cavitation at 650°C. A well developed square grain boundary pattern is present. Cavities and cracks resulting from linkage of growing cavities are present along grain boundaries. Also present are significant numbers of cavities in the interior of the grains.

DISCUSSION AND ANALYSIS

Grain boundary migration and grain boundary sliding were observed to occur during high temperature fatigue. The corresponding dislocation structures consisted of rectangular dislocation cells with the dislocation walls aligned along lines of maximum shear stresses. In regions near grain boundaries on which maximum cavitation is expected to occur (i.e., along grain boundaries aligned along lines of maximum shear), a size gradient of dislocation cells was found. Some of the dislocation cell walls in this region contained small holes which may well be cavities produced by fatigue. The presence of a size gradient of dislocation cells and the holes in the dislocation cell walls suggests a possible mechanism for grain boundary cavitation.

Dislocation Cell Size Versus Stress

At 550°C, the dislocation cell size varied from large dislocation cells in the interior of the grains to small cells near the grain boundary. The variation of dislocation cell size throughout the grains was over such a large distance that an average dislocation cell size could not be determined for a given saturation stress.

At 650°C, however, the size gradient of the dislocation cells was confined to a region near the grain boundary. At a distance of a few microns from the grain boundary, the cells were of uniform size. Thus the dislocation cell size

as a function of saturation stress could be determined at this temperature. The dislocation cell size was found to be inversely proportional to the saturation stress as indicated in Figure 20.

The linear variation of the saturation stress with the inverse of the dislocation cell size is in agreement with other investigations for Cu, Fe, and Al of cell size as a function of flow stress.[10,13-17] Staker and Holt[16] have established that the flow or saturation stress is directly proportional to the square root of the dislocation density and that the dislocation cell size is inversely proportional to the square root of the dislocation density. Consequently, the saturation stress is inversely proportional to the dislocation cell size.

To compare the results obtained with the published literature, the saturation stresses were normalized by dividing the saturation stresses by the shear modulus at 650°C and the Burgers vector. The normalized stresses and the corresponding dislocation cell sizes were found to be in good agreement with the published data compiled by Staker and Holt[16] as shown in Figure 21.

Temperature Effect on Dislocation Structures

Staker and Holt[16] found that the normalized flow stress at a given temperature is not equal to the normalized flow stress at a higher temperature of specimen with the same cellular dislocation structure: it is less at the higher

temperature because of increased thermal activation. They found the ratio of the normalized flow stresses to be equal to the Cottrell-Stokes factor.*

In this investigation, an average dislocation cell size could not be determined for a given saturation stress at 550°C. Consequently, a quantitative measure of the effect of temperature on the size of the dislocation cells could not be made.

In agreement with other investigations[16,17] of dislocation cells, the thickness of the dislocation cell walls was found to decrease as the temperature was increased. In addition to the decrease of the dislocation cell wall thickness, the alignment of the dislocation cell walls was found to change as the temperature was increased. At low temperatures, dislocation motion is confined to specific crystallographic planes and directions and hence the cell walls tend to be aligned along specific crystallographic directions.[21,22] Consequently, at low temperatures, the dislocation cell walls will not appear to be aligned along specific directions of stress.

The dislocation cell walls resulting from high temperature fatigue were found to be aligned along lines of maximum shear stresses and appeared to be independent of

---

*The Cottrell-Stokes factor is the ratio of the normalized flow stress at a given temperature to the normalized flow stress at room temperature for a given dislocation structure. It is a constant, independent of strain (i.e., the dislocation structure).

specific crystallographic planes and directions. X-ray examination, using a back-reflection technique on a rotating specimen which had been fatigued at high temperature, indicated that no preferential orientation was present in the test specimen, thus indicating that the alignment of the cell walls was indeed independent of crystallographic planes and directions.

A plot of saturation stress versus the inverse of the absolute temperature for a constant strain amplitude is shown in Figure 22. This figure indicates that two different mechanisms are operative. At low temperatures, the saturation stress is relatively independent of temperature. This is known as the athermal region.[23] In the athermal region, the ability of a metal to form dislocation cells is highly dependent on stacking fault energy. If the stacking fault energy is high, dislocations can cross slip easily and dislocation cells will form rather than planer dislocation arrays.[9,10] The dislocation cells thus formed will tend to be of a crystallographic nature.[21,22]

At high temperatures, the saturation stress is very sensitive to changes in temperature (Fig. 22). Due to the occurrence of diffusion controlled dislocation climb, dislocation motion will not be confined to specific crystallographic planes or directions. Thus a metal which will deform by planer slip at low temperatures (i.e., will not form dislocation cells), will form a cellular structure at high temperatures.[19] The cellular structure formed

at high temperatures will be sensitive to the superimposed stress system and the dislocation cell walls will align themselves along lines of maximum shear stresses.

Dislocation Cell Size Gradient

Near grain boundaries which were aligned along lines of maximum shear stresses, a size gradient of dislocation cells was found (Figs. 11, 12). Near grain boundaries which were not aligned along lines of maximum shear stresses, a size gradient of dislocation cells was not observed (Fig. 14). Grain boundaries which are aligned along lines of maximum shear stresses experience a greater rate of sliding than grain boundaries which are not.[20,24] Thus it can be concluded that the size gradient of dislocation cells is present along grain boundaries which are sliding.

By assuming that at constant temperature the local flow stress is proportional to the inverse of the dislocation cell size, a plot of the inverse of the dislocation cell size as a function of distance from the grain boundary would indicate the stress as a function of distance from the grain boundary. This is shown in Figure 23. The higher stresses present near the grain boundary and the correspondingly greater amounts of plastic deformation in this region are consistent with the observation that grain boundary sliding is not confined to the grain boundary but occurs in a finite shear zone on either size of the grain

boundary.[20,24,25]

The temperature and stress dependence of the size of the shear zone is indicated in Figure 23. The width of the shear zone was found to decrease as the saturation stress was increased. As the temperature is increased, the width of the shear zone is decreased. The reason for this behavior could not be explained satisfactorily.

Mechanism of Grain Boundary Cavitation

Greenwood[27] first suggested that creep deformation within the grains creates an excess concentration of vacancies which diffuse towards the grain boundaries. The excess concentration of vacancies at the grain boundaries is responsible for the growth of grain boundary cavities. Skelton[28] made a detailed analysis of grain boundary cavitation in fatigue based on this model. He suggested that the vacancies reach the cavities from a "lifetime" sphere around the cavities. The number of vacancies is proportional to the strain rate. The net number of vacancies was proportional to the rate of production minus the rate of annihilation.

Broomfield[30] suggested that the main flux of vacancies responsible for grain boundary cavitation comes from the grain boundary itself.

Gittins[3] has suggested that cavity growth may be interpreted on the basis of a model in which defects absorbed by grain boundary migration contribute to cavity growth. The

model is based on the premise that extensive grain boundary migration occurs continuously throughout the fatigue process. This premise is contradictory to the results obtained by Westwood and Taplin[5] and by Skelton[29] who found that the onset of cavitation coincided with the attainment of a stable grain boundary configuration.

A dislocation cell size gradient was observed near sliding grain boundaries during high temperature fatigue. Small holes were observed in the dislocation cell walls in this region. On the basis of these observations, the following mechanism of grain boundary cavitation is proposed as an alternative to the above mechanisms.

The observed decrease in the thickness of the dislocation cell walls with increasing temperature suggests that the majority of the dislocation reactions are confined to a region near and inside the dislocation cell walls. Therefore, it is postulated that the vacancies resulting from deformation (e.g., mutual annihilation of edge dislocations) are produced within the cell walls and diffuse very short distances to sinks located within the dislocation boundary.[26] When the rate of vacancy production exceeds the ability of the existing sinks to annihilate these extra vacancies, new sinks in the form of cavities will be nucleated which grow by further condensation of vacancies.

The above consideration of vacancy production suggests that cavities will nucleate and grow on any dislocation boundary where a larger concentration of vacancies is

produced than the existing sinks are able to annihilate. The preferential nucleation sites will be regions of high dislocation density within the cell walls.

Consider the rate of cavity growth in a unit weight of metal. Saada[26, p.427] has suggested that the concentration of vacancies produced by mechanical work is proportional to the work done. Assuming that this relationship is valid for a cellular dislocation structure, the concentration of vacancies for a given amount of mechanical work will be:

$$dc = \frac{A}{G} \int_0^{\varepsilon_p} \sigma d\varepsilon \qquad (3)$$

where dc = incremental concentration of vacancies, A = constant at constant temperature, and G = shear modulus.

In order to calculate the concentration of vacancies produced in a unit weight of metal during one fatigue cycle, the amount of work done per cycle must be known (i.e., the area of the hysteresis loop produced by plotting stress versus plastic strain). Morrow[8] has demonstrated that the shape of the hysteresis loop can be mathematically represented quite accurately by the same power law function used to approximate the cyclic stress-strain curve. Using this approximation, Morrow showed that the work done per fatigue cycle was equal to the following expression:

$$\Delta W = 2\sigma_a \Delta\varepsilon_p \left(\frac{1-n}{1+n}\right) \qquad (4)$$

where ΔW = work per unit weight of metal done per cycle,

σ_a = stress amplitude, $\Delta\varepsilon_p$ = plastic strain amplitude, and n = cyclic strain hardening exponent. Thus the concentration of vacancies produced in a unit weight of metal per cycle will be:

$$C = \text{const.}\ \Delta\varepsilon_p \cdot \sigma_a \tag{5}$$

The concentration of vacancies at time t will be:

$$C = B(f,T) \cdot t \cdot \sigma \cdot \Delta\varepsilon_p \tag{6}$$

where B is a function of temperature and cyclic frequency.

When the rate of vacancy production is low, the existing sinks will be able to annihilate the vacancies produced. Once a critical rate of vacancy production is exceeded, cavities will be nucleated and grow. Thus the growth will be expressed by:

$$V = B(f,T) \cdot (\Delta\varepsilon_p - \Delta\varepsilon_c) \cdot t \cdot \sigma_a \tag{7}$$

where V = void volume per unit weight of metal, $\Delta\varepsilon_c$ = critical amount of plastic deformation required to produce critical concentration of vacancies, t = time, B = constant at constant temperature and frequency, and σ_a = stress amplitude.

The number of vacancies produced is proportional to the mechanical work. Therefore, the cavity volume increase per cycle is proportional to the work. Because the work per cycle is constant at saturation, the cavity volume increases as a linear function of time.

The above derivation has assumed that the stress and plastic strain amplitude remain constant throughout the time interval t (i.e., steady-state conditions prevail). This functional equation is consistent with the experimental results obtained by Gittins[3] for small values of plastic strain amplitudes and small stresses (i.e., steady-state conditions). In agreement with the experimental findings of Gittins,[3] the equation predicts that at constant plastic strain amplitude, the volume change will be linear with time, and that the rate of void growth is not a linear function of the plastic strain amplitude.

To predict on which dislocation boundaries the cavities will be first nucleated and grow preferentially, the dislocation boundaries throughout the individual grains must be considered. The dislocation cells contained in the shear zone near a sliding grain boundary are smaller than those in the centre of the grain. This indicates that more work is being done in this region of the grain and the above model predicts that cavities will be first nucleated in this region and will grow faster than those which may be nucleated elsewhere. At high strain amplitudes and high temperatures, appreciable deformation will occur in the central regions of the grains. Under these conditions, the model predicts that cavities will be nucleated and will grow also in the central regions of the grains. Thus the model is able to account for the existance of cavities within the grains.

In the model of grain boundary cavitation described, the lifetime of the individual vacancies is of secondary importance. The vacancies are generated in the dislocation cell walls and diffuse only short distances inside the cell walls to vacancy sinks located in the cell walls.

Since the rate of cavity growth depends on the diffusion of vacancies over short distances inside the dislocation cell walls, the activation energy for the rate of void growth per unit weight of metal would be expected to be equal to the activation energy for dislocation cell wall self-diffusion. Gittins[3] found that the activation energy for the rate of void growth in the high temperature fatigue of copper was slightly higher than the activation energy for grain boundary self-diffusion. This would indicate that the vacancies are confined to the dislocation cell walls where a slightly higher activation energy than that required for grain boundary self-diffusion would be required.

The cavities described by the above mechanism will form on any dislocation boundary in the grains. The existance of the dislocation cell size gradient near sliding grain boundaries means that more mechanical work is being done in this region and that the rate of cavity nucleation and growth will be proportionally higher near sliding grain boundaries. The rate of cavity growth and nucleation will be highest on grain boundaries which experience a maximum rate of sliding (i.e., on grain boundaries aligned along lines of maximum shear stresses).

SUMMARY AND CONCLUSIONS

1. At 650°C, the dislocation cell size resulting from high temperature fatigue was found to be a linear inverse function of the saturation stress.
2. At 550°C and 650°C, the dislocation cell walls were aligned along lines of maximum shear stresses and appeared to be independent of crystallographic directions.
3. Near grain boundaries which were aligned so that a maximum rate of grain boundary sliding would occur, a size gradient of dislocation cells was found. The size of the shear zone (region which contained the dislocation cell size gradient) was found to decrease as the temperature was increased and as the saturation stress was increased.
4. Small holes in the dislocation cell walls, which may have been due to high temperature fatigue, were found near the grain boundaries.
5. From the above observations, a vacancy mechanism of cavity formation is proposed which predicts that cavities will grow preferentially near sliding grain boundaries.
6. The proposed mechanism also predicts that at high stresses and temperatures, some cavities will be nucleated and grow in the interior of the grains.

7. Using the proposed mechanism, the following functional relationship was derived:

$$V = B(f,T)\cdot(\Delta\varepsilon_p - \Delta\varepsilon_c)\cdot t\cdot\sigma_o$$

This relationship shows that for steady-state conditions, void growth for a constant strain amplitude is linear with time, and that the rate of cavity growth is not directly proportional to the value of the plastic strain amplitude. The proposed equation is only applicable for small values of stress and plastic strain amplitudes (i.e., steady-state conditions).

REFERENCES

1. Williams, H.D., and Corti, C.W., Metal Sci. J., 2, 1968, p. 28.
2. Evans, H.E., and Skelton, R.P., Metal Sci. J., 3, 1969, p. 157.
3. Gittins, A., Metal Sci. J., 2, 1968, p. 114.
4. Gittins, A., Metal Sci. J., 2, 1968, p. 51.
5. Westwood, J., and Taplin, D.M.R., paper presented at Can. Conf. of Metallurgists, Montreal, 1971.
6. Gollard, D.I., and Beevers, C.J., Metal Sci. J., 5, 1971, p. 174.
7. Gifkins, R.C., Fracture, ed. C.J. Osborne, U. of Melbourne, 1965.
8. Morrow, JoDean, Internal Friction, Damping and Cyclic Plasticity, ASTM STP 378, 1964, p. 45.
9. Feltner, C.E., and Laird, C., Acta Met., 15, 1967, p. 1621.
10. Feltner, C.E., and Laird, C., Acta Met., 15, 1967, p. 1633.
11. Johnston, T.L., and Feltner, C.E., Met. Trans., 1, 1970, p. 1161.
12. Thompson, A.W., and Backofen, W.A., Acta Met., 19, 1971, p. 597.
13. Abdel - Raouf, H., Benham, P.P., and Plumtree, A., Can. Met. Quarterly, 10, 1971, p. 87.

14. Pratt, J.E., Acta Met., 15, 1967, p. 319.

15. Abdel-Raouf, H., and Plumtree, A., Met Trans, 2, 1971, p. 1863.

16. Staker, M.R., and Holt, D.L., Acta Met., 20, 1972, p. 569.

17. McQueen, J.H., Wong, W.A., and Jones, J.J., Can. J. of Physics, 45, 1967, p. 1225.

18. Vandervoot, R.R., Trans. AIME, 245, 1969, p. 2269.

19. Oblak, J.M., and Owczarski, W.A., Met. Trans., 3, 1972, p. 617.

20. Walter, J.L., and Cline, H.E., Trans. AIME, 242, 1968, p. 1823.

21. Laufer, E., Czechoslavak Journal of Physics, B19, 1969, p. 333.

22. Gostelow, C.R., Met. Sci. J., 5, 1971, p. 177.

23. Gorman, J.A., Wood, D.S., and Vreeland, T. Jr., J. of App. Phys., 40, 1969, p. 833.

24. Puttick, K.E., and Tuck, B., Acta Met., 13, 1965, p. 1043.

25. McLean, D., Grain Boundaries in Metals, Clarendon Press, Oxford, 1957.

26. Van der Beakel, A., Vacancies and Interstitials in Metals, ed. A. Seeger, Am. Elsevier Pub. Co., 1968.

27. Greenwood, J. Iron and Steel Inst., 20, 1952, p. 274.

28. Skelton, R.P., Phil. Mag., 14, 1966, p. 563.

29. Skelton, R.P., Met. Sci. J., 1, 1967, p. 140.

30. Broomfield, Ph. D. Thesis, Cambridge, 1965.

TABLE 1

ANALYSIS OF NICKEL

Element	Content (ppm)
As	<1
Ag	<0.4
Al	10
Ba	<8
B	<50
C	100
Ca	<6
Cd	<25
Co	220
Cr	1
Cu	9
Fe	<20
Mg	2
Mn	<4
Mo	<8
Pb	<20
S	3-8
Se	1
Si	<11
Sn	<25
Te	<1
Ti	<10
Zn	<50
O_2	32

TABLE 2

ANALYSIS OF ULTRA HIGH PURITY NITROGEN

Ar	7 ppm
O_2	<3 ppm
CO_2	nil
H_2O	<3 ppm
N_2	balance

Fig. 1 Example of grain boundary cavitation in Ni fatigued at 600°C.
200x Mag.

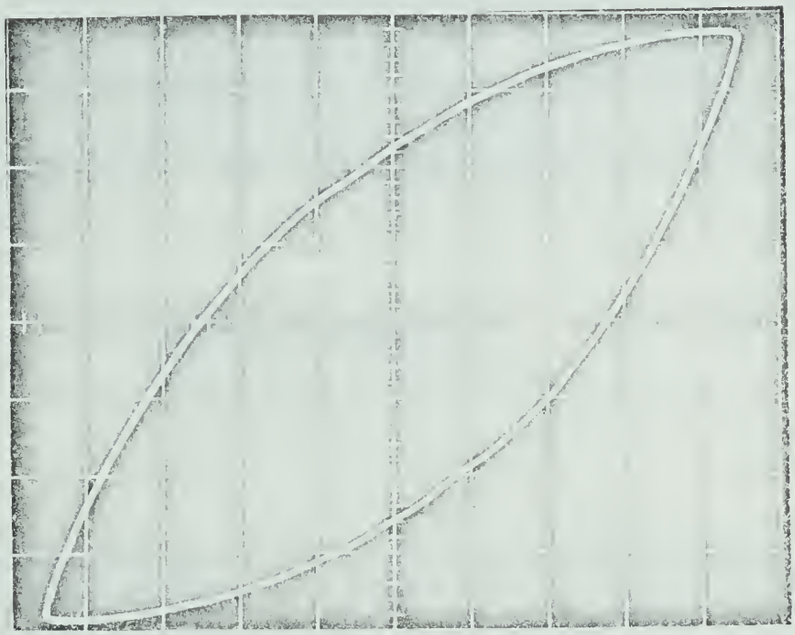

Fig. 2 Stabilized hysteresis loop. Vertical axis is the stress axis and horizontal axis is the strain axis. The width of the loop at zero stress is the plastic strain amplitude.

Fig. 3 Nickel test specimen (actual size).

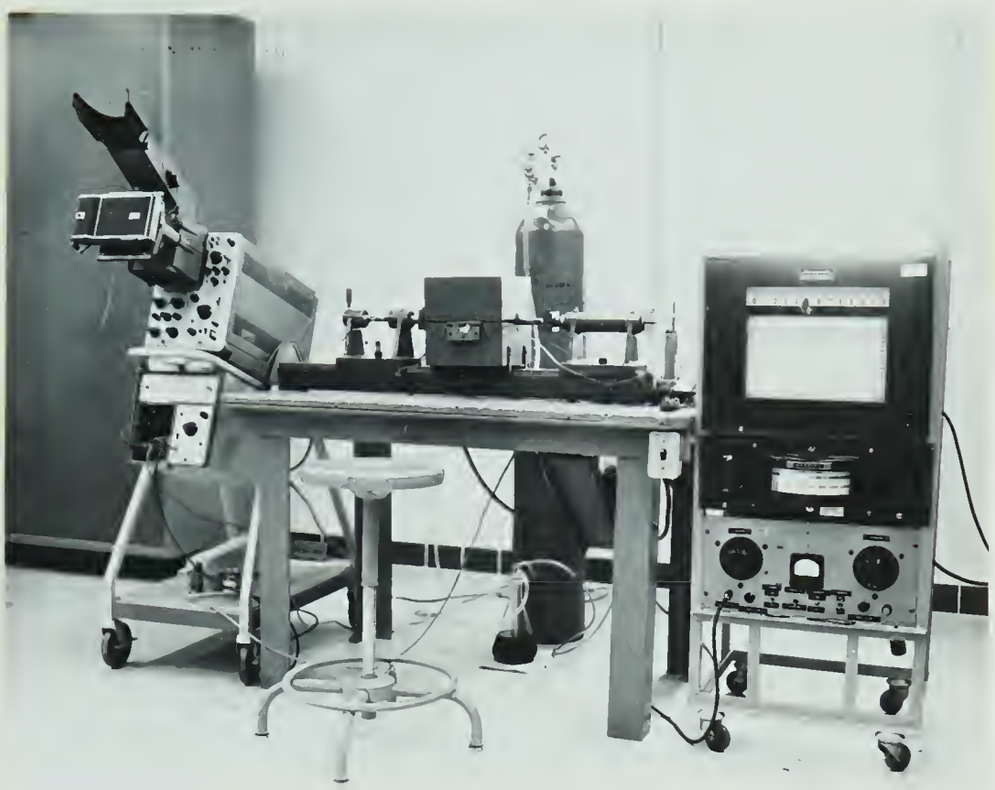

Fig. 4 Torsion fatigue machine.

Fig. 5 Fatigue specimen in specimen grips with stainless steel atmospheric chamber.

Fig. 6 Plastic surface replica of a specimen fatigued at 550°C and a total shear strain of .005. The arrows indicate directions of maximum shear stresses. 112x Mag.

Fig. 7 Plastic surface replica of a specimen fatigued at 650°C and a plastic shear strain amplitude of .003. The arrows indicate directions of maximum shear stresses.
112x Mag.

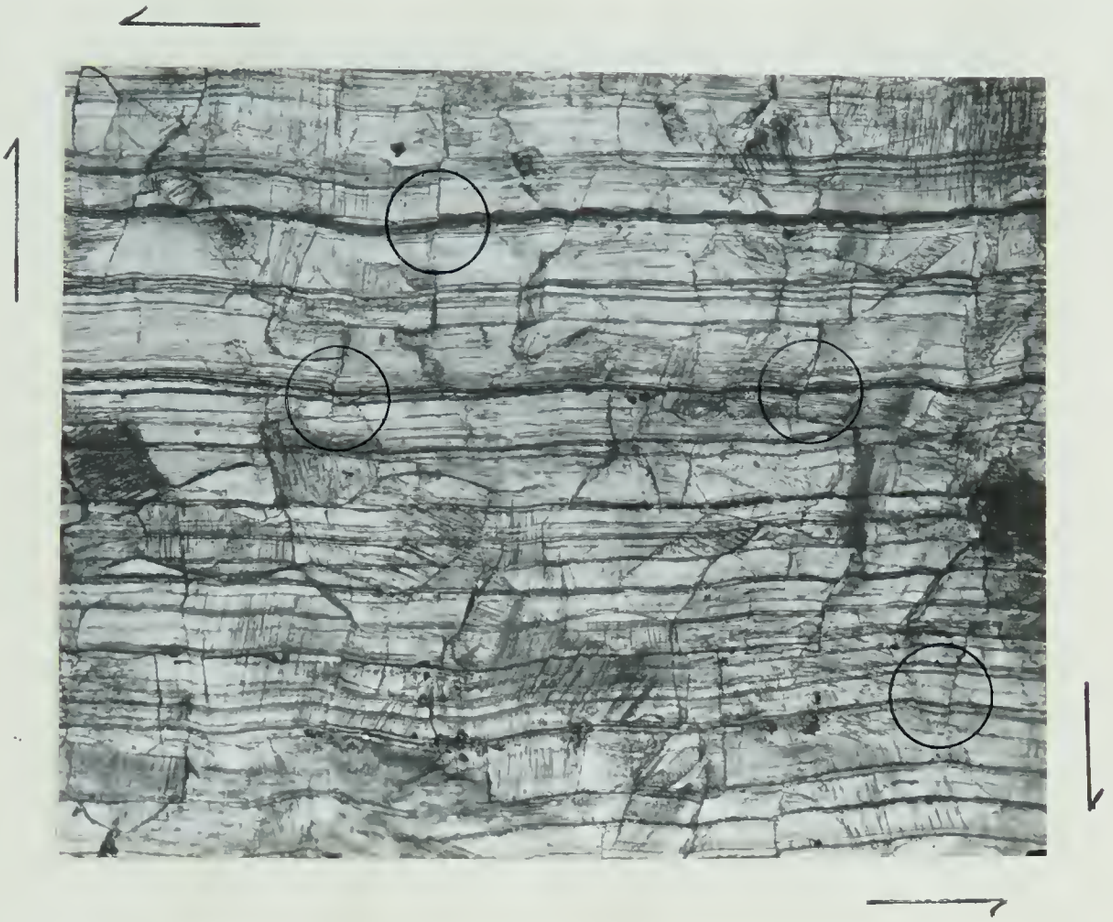

Fig. 8 Plastic surface replica of a specimen fatigued at 650°C and a plastic shear strain smplitude of .013. The arrows indicate the directions of maximum shear stresses. The circles show examples of grain boundary sliding. 112x Mag.

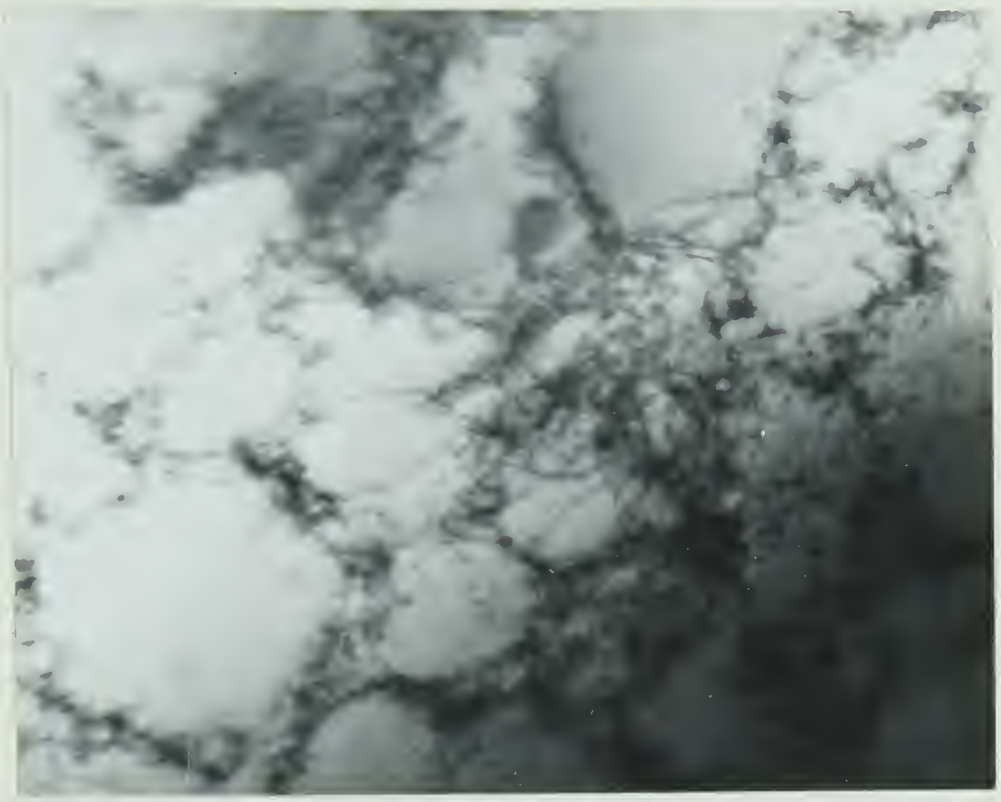

Fig. 9 Transmission electron micrograph of a specimen fatigued at room temperature and a total shear strain amplitude of .002.
16,800x Mag.

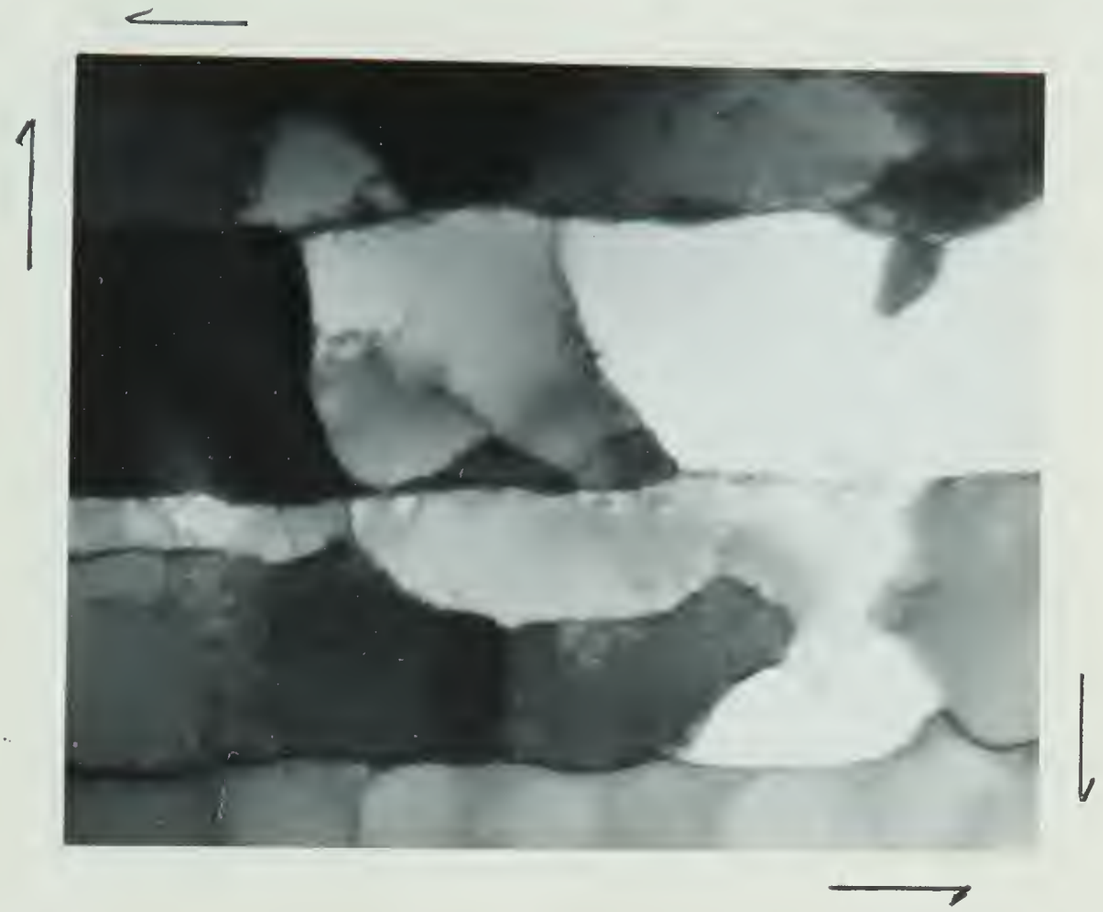

Fig. 10 Transmission electron micrograph of a specimen fatigued at 650°C and a plastic shear strain amplitude of .013. The arrows indicate the directions of maximum shear stresses.
12,600x Mag.

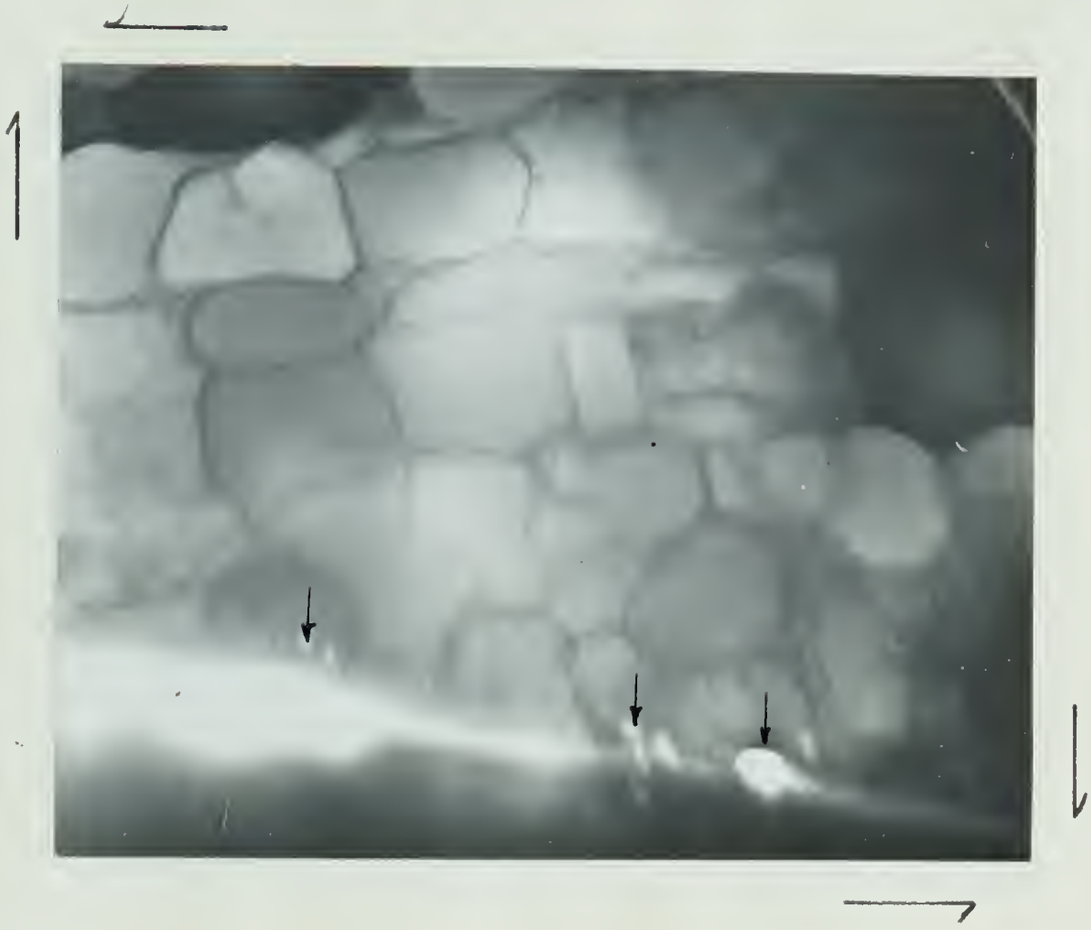

Fig. 11 T.E.M. of a specimen fatigued at 550°C and a plastic shear strain amplitude of .013. The arrows indicate the directions of maximum shear stresses. Note the appearance of small holes near the grain boundary.
7500x Mag.

Fig. 12 T.E.M. of a specimen fatigued at 650°C and a plastic shear strain amplitude of .003 showing the dislocation cell size gradient near a grain boundary. 7500x Mag.

Fig. 13 T.E.M. of a specimen fatigued at 650°C and a plastic shear strain amplitude of .003 showing detail of dislocation structure near grain boundary shown in Fig. 12.
28,000x Mag.

Fig. 14 T.E.M. of a specimen fatigued at 550°C and a shear strain amplitude of .013. The arrows indicate the directions of maximum shear stresses.
19,500x Mag.

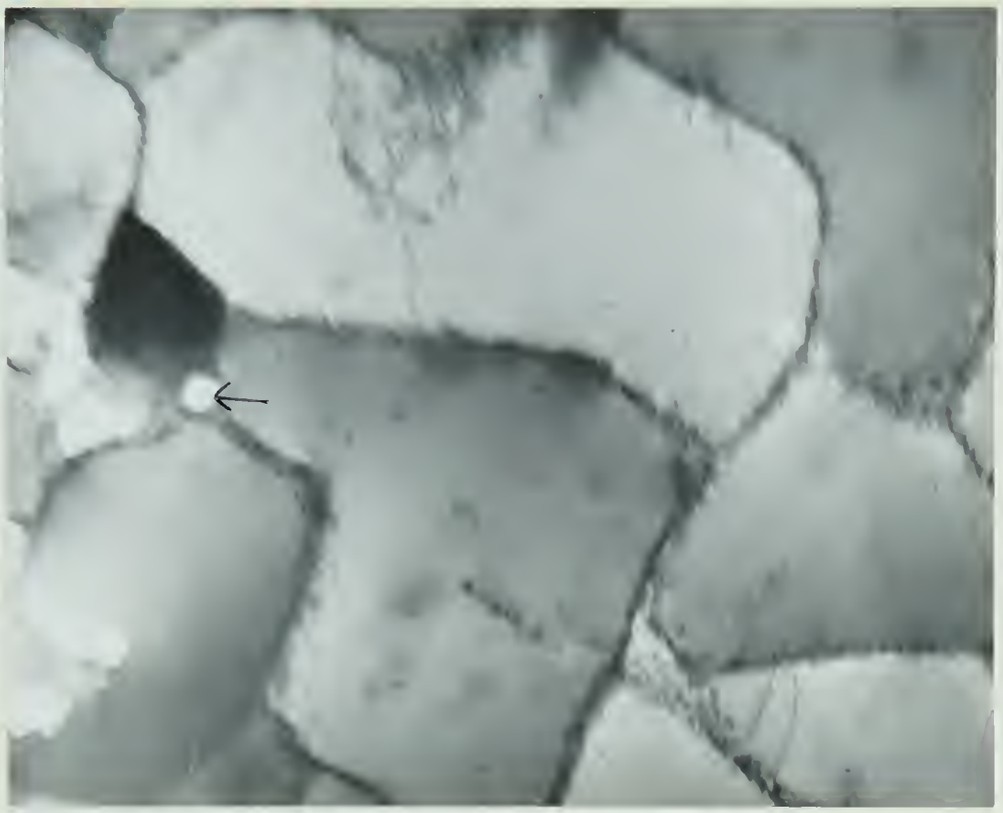

Fig. 15 T.E.M. of a specimen fatigued at 550°C and a shear strain amplitude of .013. Note the holes in the thin foil at the dislocation cell walls.
13,300x Mag.

Fig. 16 T.E.M. of a specimen fatigued at 650°C and a plastic shear strain amplitude of .013. Note the holes in the thin foil at the dislocation boundary. 58,500x Mag.

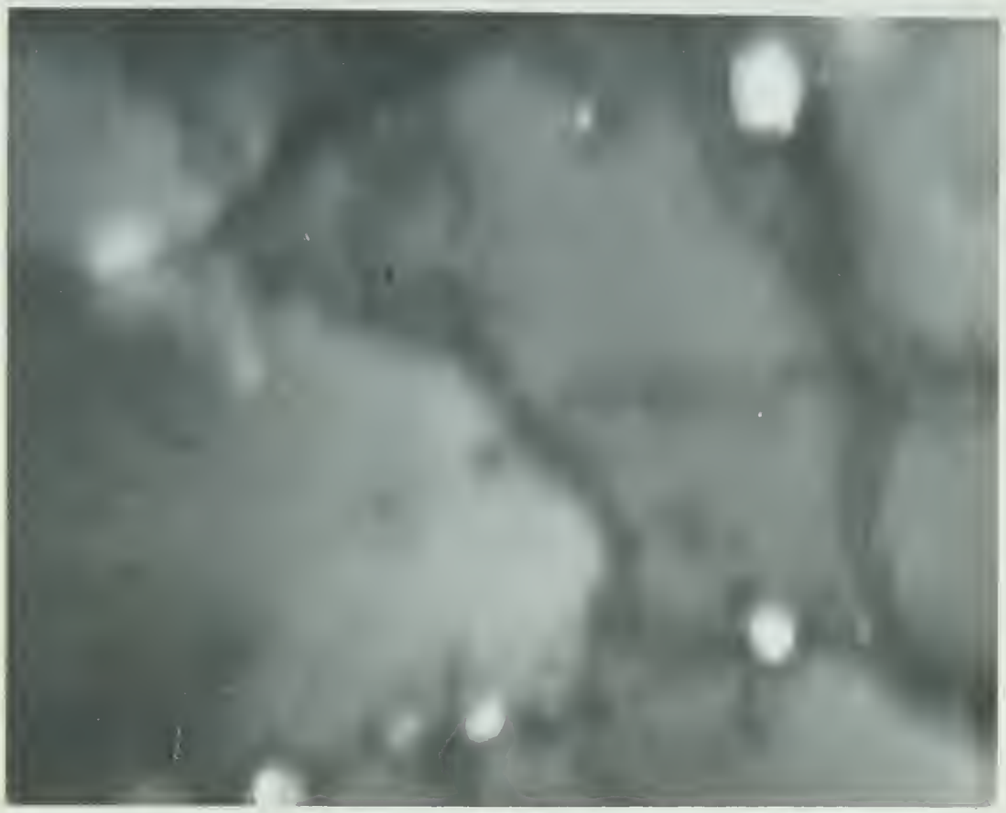

Fig. 17 T.E.M. of a specimen fatigued at 650°C and a plastic shear strain amplitude of .013. Note the holes in the thin foil at the dislocation cell walls. 68,000x Mag.

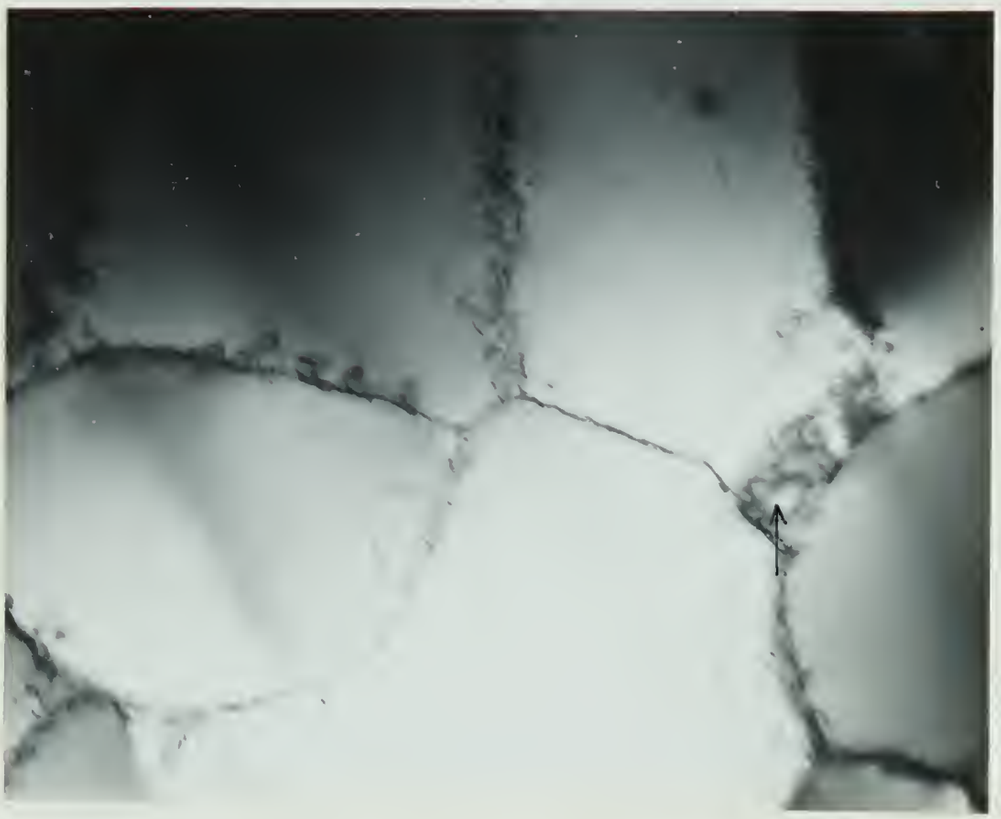

Fig. 18 T.E.M. of a specimen fatigued at 650°C and a plastic shear strain amplitude of .013. Note the cavity in a region of high dislocation density.
18,300x Mag.

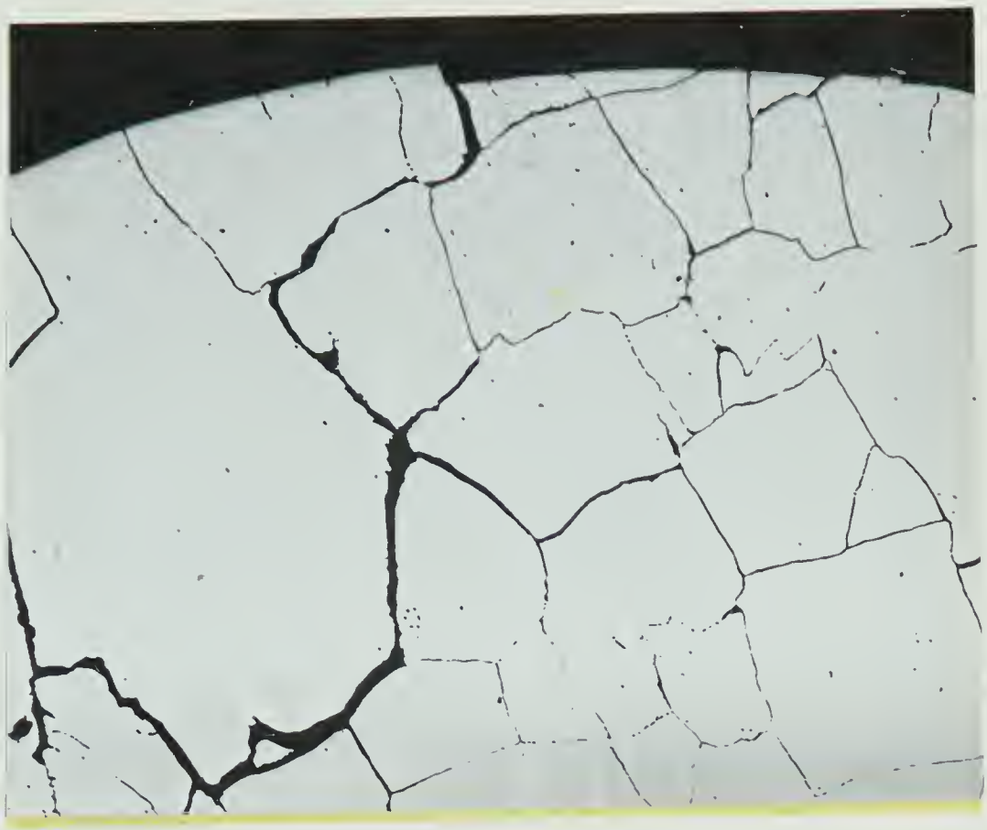

Fig. 19 Microstructure of a fatigue failure as a result of grain boundary cavitation. A square grain boundary pattern, cavities and cracks resulting from linkage of cavities along the grain boundaries are present. Also note the presence of small cavities in the interior of the grains.
Etchant: dilute Marbles Reagent.
50x Mag.

Fig. 20

SATURATION STRESS vs. INVERSE of DISLOCATION CELL SIZE

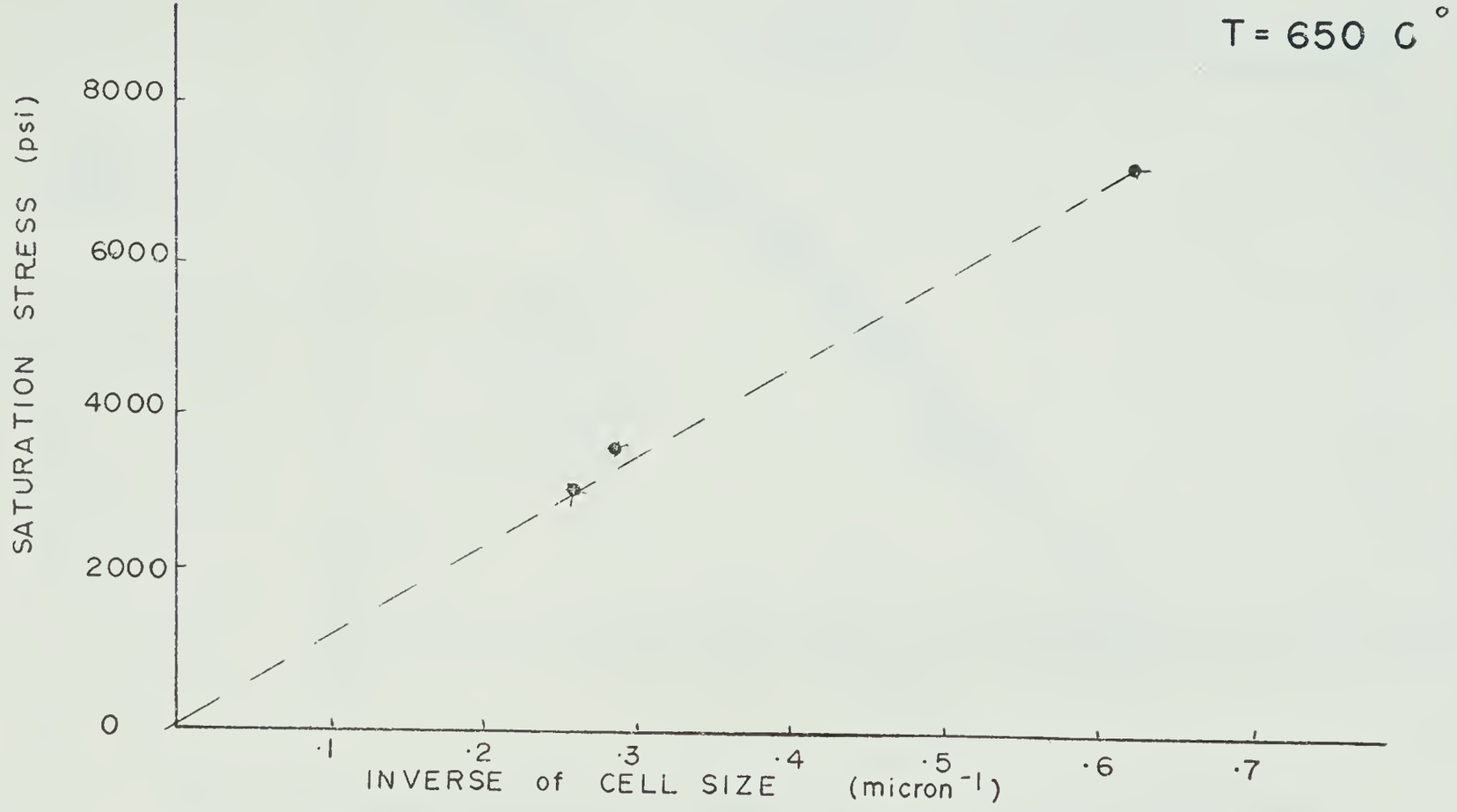

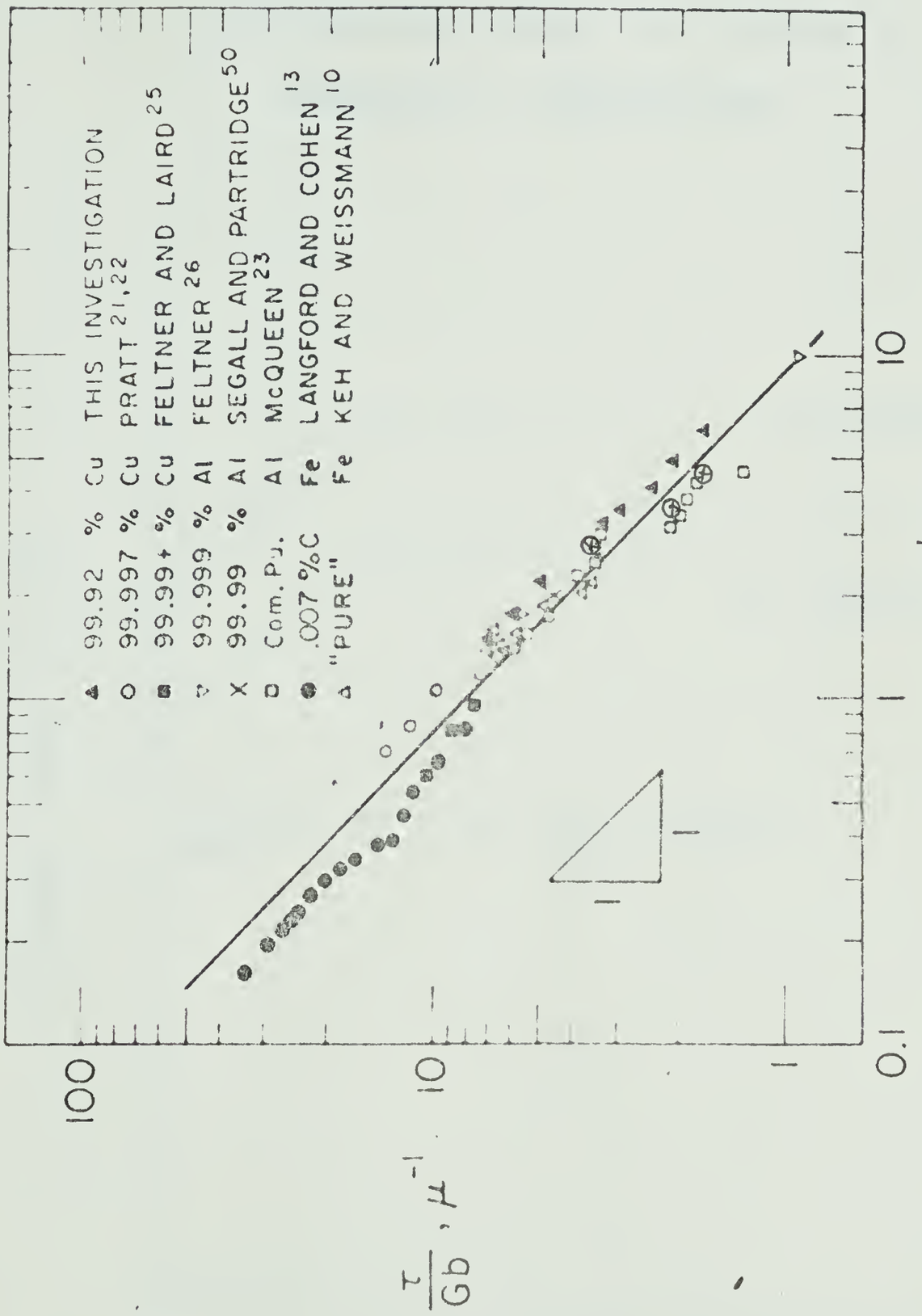

Fig. 21 From Reference 16, data compiled by Staker and Holt. Data from this investigation shown as ⊗.

Fig. 22

SATURATION STRESS vs. INVERSE of ABSOLUTE TEMPERATURE

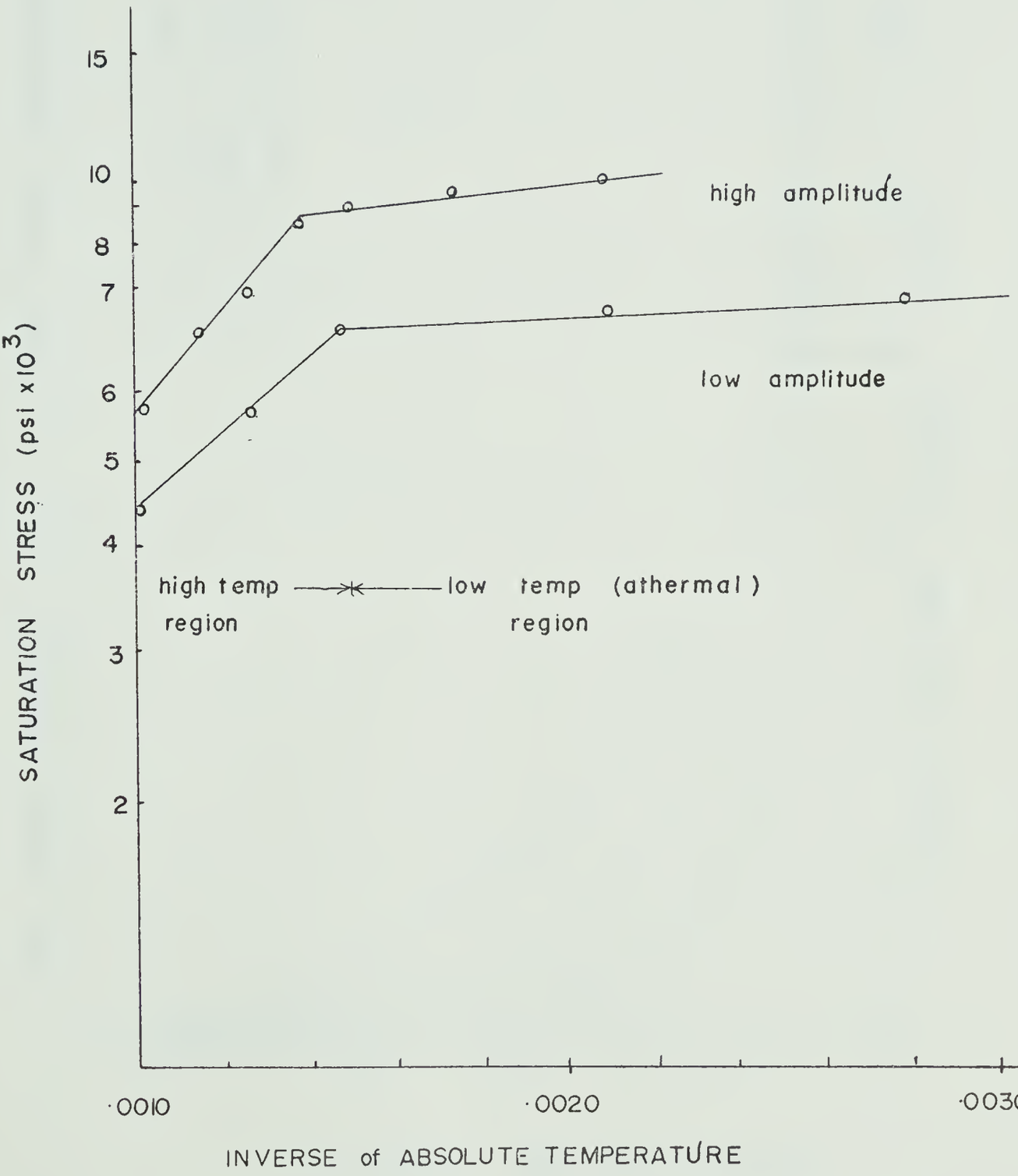

Fig. 23

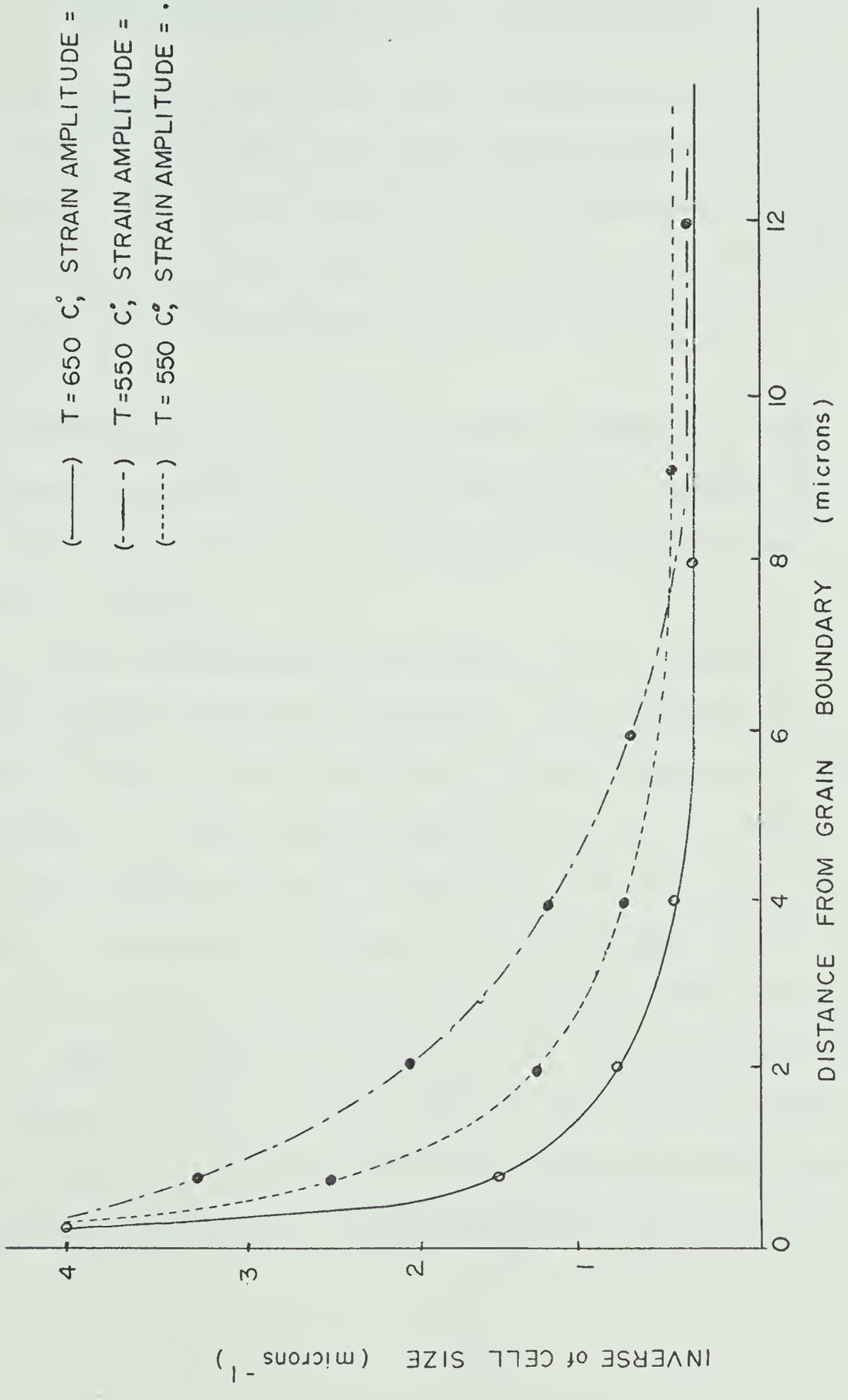
CELL SIZE GRADIENT NEAR A SLIDING GRAIN BOUNDARY
(——) T = 650 C°; STRAIN AMPLITUDE = 0.003
(-—-—-) T=550 C°; STRAIN AMPLITUDE = 0.003
(------) T = 550 C°; STRAIN AMPLITUDE = .013
INVERSE of CELL SIZE (microns^{-1})
DISTANCE FROM GRAIN BOUNDARY (microns)
0
2
4
6
8
10
12
1
2
3
4

APPENDIX I

Calibration of Fatigue Testing Machine

The torsional load cell was calibrated by putting a moment arm on the load cell and hanging weights from the moment arm. The known torque was then measured using a Tektronix carrier amplifier. The torque-strain calibration curve for the torsional load cell is shown in Figure AII-1.

The angle of twist of the machine could be varied by moving an eccentric on the loading arm. Figure AII-2 shows the angle of twist in one direction versus the eccentric setting.

At test temperature, the grips of the testing machine deform significant amounts. To calculate the amount of twist in the grips for a given stress at test temperature, a solid dummy specimen made of stainless-steel was inserted into the grips and the twist of the grips as a function of stress at a given temperature was found for a series of temperatures ranging from 200°C to 650°C. This is shown in Figure AII-3. To calculate the true angle of twist of the specimen, the angle of twist of the grips at a given stress and temperature was subtracted from the angle of twist measured from the loading arm.

Fig. AII-1

TORQUE-STRAIN CALIBRATION FOR TORSIONAL LOAD CELL

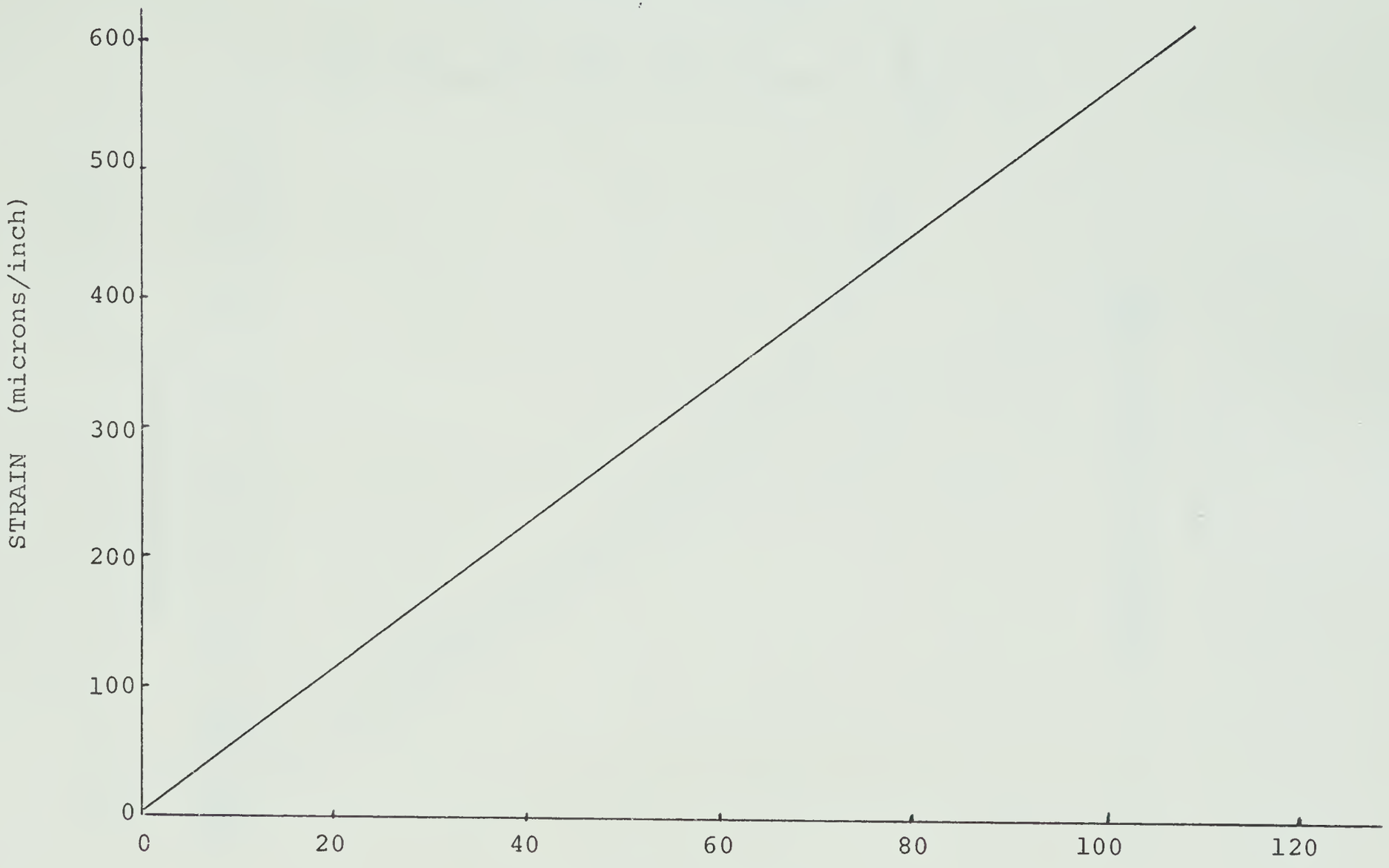

(Line drawn from statistical data)

Fig. AII-2

TWIST ANGLE OF ECCENTRIC

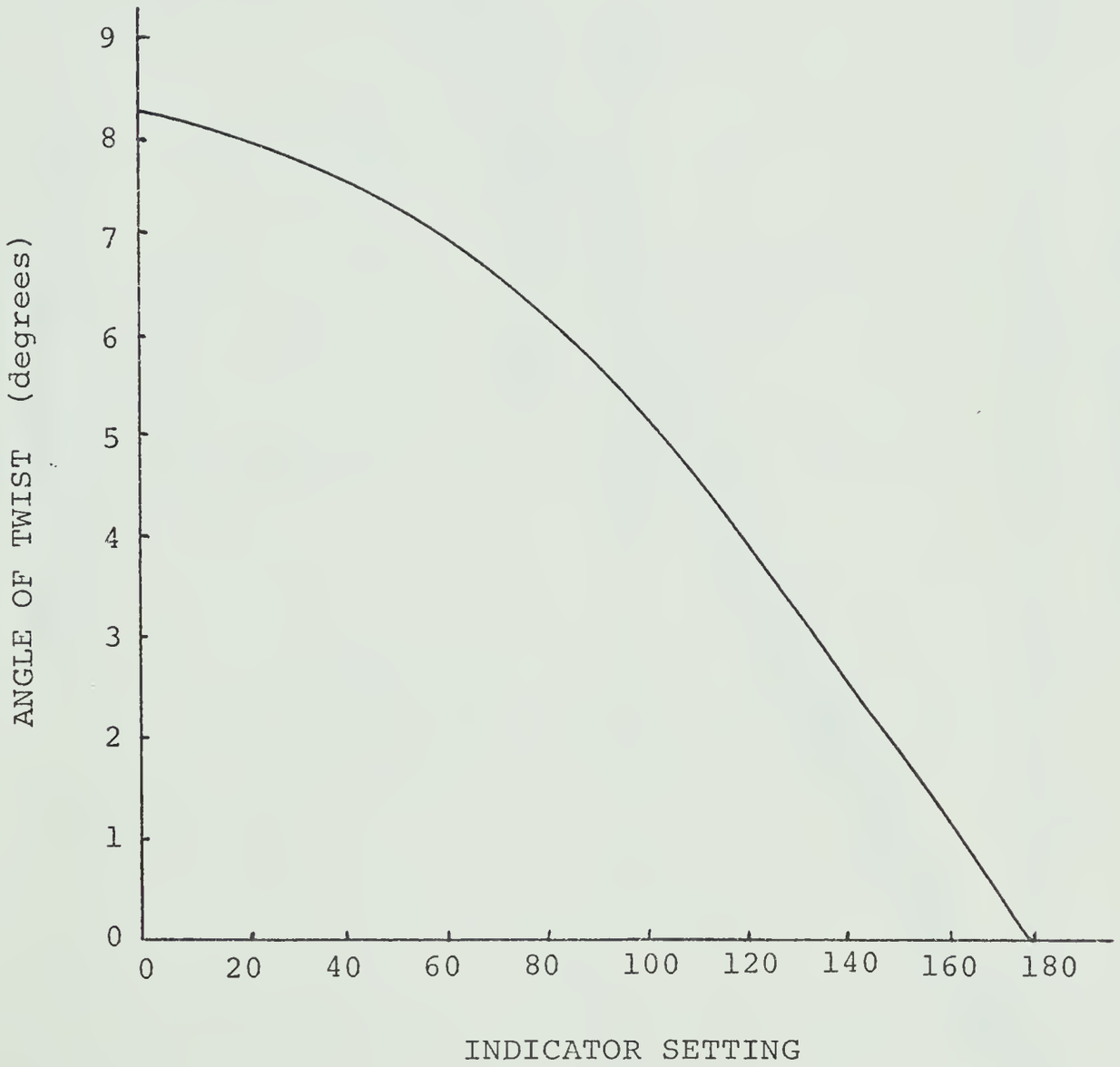

Fig. AII-3

TWIST OF GRIPS VERSUS TORQUE

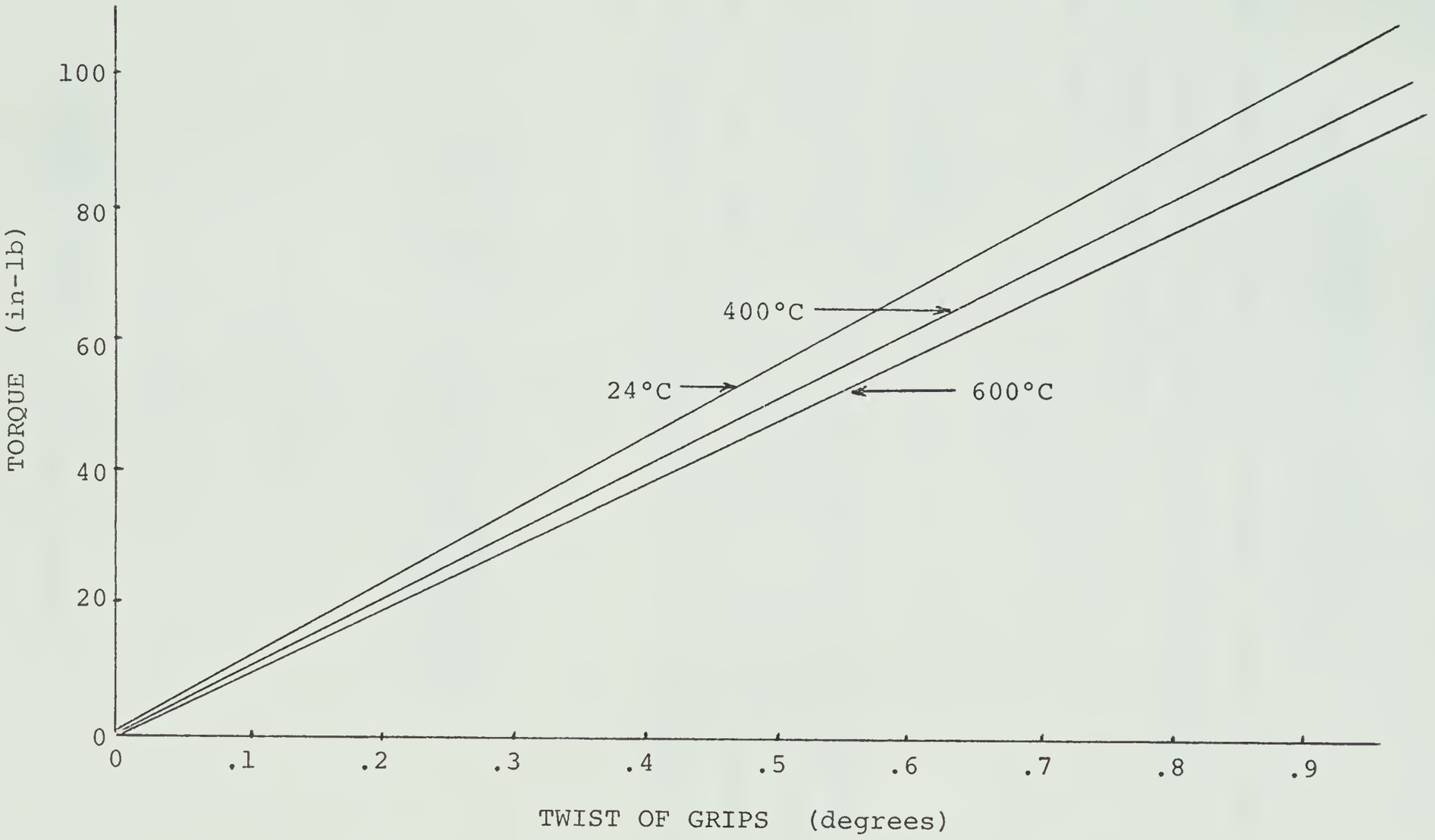

APPENDIX II

Calculation of Stress in Reverse Torsion Fatigue Specimens

The saturation stress at the outside surface of the fatigue specimens was calculated at test temperatures using the formula derived below.

For pure shear:

$$T = \int_{area} \tau \rho da$$

T = torque
ρ = radius
τ = shear stress

At small angles of twist, the specimens were assumed to deform by pure shear. At saturation, the forward stress is equal to the reverse stress. Since inelastic deformation was occuring, a non-linear stress-strain function was assumed.

$$\tau = \tau_o \gamma^m$$

τ = shear stress
τ_o = a constant at constant temperature
γ = total shear strain in one direction
m = a constant at constant temperature

Therefore

$$T = \int_{area} \tau_o \gamma^m \rho da$$

But

$$\gamma = \frac{\theta \rho}{L}$$

ρ = radius
L = gage length
θ = angle of twist in one direction

Therefore

$$T = \int_0^r \tau_o \left(\frac{\theta}{L}\right)^m \rho^{m+1} da$$

For a circular cross-section

$$da = 2\pi\rho d\rho$$

and

$$T = \int_0^r \tau_o \left(\frac{\theta}{L}\right)^m 2\pi \int^r \rho^{m+2} d\rho$$

$$T = \frac{\tau_o \left(\frac{\theta}{L}\right)^m 2\pi r^{m+3}}{m+3}$$

But

$$\tau = \tau_o \left(\frac{\theta r}{L}\right)^m$$

Therefore

$$T = \frac{\tau 2\pi r^3}{m+3}$$

Since

$$J = \frac{\pi r^4}{2}$$

Therefore

$$\tau = \frac{Tr(m+3)}{4J}$$

r = outside radius

When the stress versus strain is a linear function, m = 1 and the above formula simplifies to the following form:

$$\tau = \frac{Tr}{J}$$

The experimental value of m at a given test temperature was determined by plotting the log of the torque at saturation versus the log of the angle of twist at the test temperature. A single specimen was used to determine the experimental value of m.

Thus the stresses at the outside surface of the fatigue specimens were calculated using the experimental values of m and setting $J = \frac{\pi}{32}(D_o^4 - D_i^4)$.

The experimental values of m were .25 at 550°C and .37 at 650°C.

APPENDIX REFERENCES

1. Seely, B. and Smith, J.O., Advanced Mechanics of Materials, 2nd ed., John Wiley & Sons (1967).

2. Nash, W.A., Theory and Problems of Strength of Materials, Schaum Publishing Co. (1957).